photonics

MDPI

Communication

Investigation into Electromagnetic Compatibility Conducted Susceptibility of a Laser Ranging System

Peng Huang [1], Bing Li [1,*], Weimin Li [2], Yi Liao [3] and Donglin Su [1,*]

[1] Research Institute for Frontier Science, School of Electronic and Information Engineering, Beihang University, Beijing 100191, China
[2] China Academy of Launch Vehicle Technology, Beijing 100191, China
[3] Shanghai Radio Equipment Research Institute, Shanghai 201109, China
* Correspondence: bingli@buaa.edu.cn (B.L.); sdl@buaa.edu.cn (D.S.)

Abstract: Laser ranging systems are a widely used form of electronic system and are generally influenced by complex electromagnetic environments. We used a laser ranging system comprising the VL53L0X laser ranging sensor module as the research object and designed a sensitive experimental platform based on the laser ranging system. In this work, we have shown that electromagnetic interference signals can affect the performance of laser ranging systems. The electromagnetic interference signal was found to enter through the chip selection port of the laser sensor chip to affect the work of the laser sensor chip. Finally, we obtained the susceptibility threshold characteristics of the laser ranging system under the influence of different types of interference signal. This study deepens the understanding of the electromagnetic susceptibility mechanism of laser ranging systems and helps in the design of their electromagnetic compatibility.

Keywords: bulk current injection (BCI); electromagnetic environmental effect; electromagnetic interference; susceptibility threshold; laser ranging; laser sensor

Citation: Huang, P.; Li, B.; Li, W.; Liao, Y.; Su, D. Investigation into Electromagnetic Compatibility Conducted Susceptibility of a Laser Ranging System. *Photonics* **2023**, *10*, 397. https://doi.org/10.3390/photonics10040397

Received: 18 February 2023
Revised: 23 March 2023
Accepted: 27 March 2023
Published: 3 April 2023

1. Introduction

With the development of electronic information technologies, the complexity of the electromagnetic environment has increased. Electromagnetic compatibility is an important ability of electronic information systems. It is a fundamental prerequisite for electronic information systems to have the ability to adapt to the electromagnetic environment [1–3]. Laser ranging is a non-contact measurement method, which is widely used in electronic measurement systems [4–7]. Compared with other non-contact distance measurement methods, laser ranging has the characteristic of a long measurement distance and is gaining attention in various application fields, especially for use in the increasingly intelligent future society. Laser-ranging systems are widely used in autonomous vehicles [8–12], the military field of laser guidance [13], unmanned aerial vehicles [14,15], geoscience and remote sensing [16], laser power transmission [17,18], virtual reality, aerospace and other fields [19]. The stability of laser systems is also receiving growing attention. Related studies have focused on the laser stability characteristics of ytterbium-doped triple-clad laser fibers [20] on laser energy fluctuations [21], on a stabilized, coherent, narrow-linewidth, Brillouin random-fiber laser with low lasing noise [22], on the thin disk-shaped structure with a multi-pass pumping scheme that can stabilize the laser mode, beam quality and efficiency [23], and on other aspects of laser stability [24–28]. Almost all the cited references are related to the reliability of laser systems and how to improve their performance. However, no one has studied the changes in the performance of laser systems when faced with electromagnetic interference, nor has anyone studied the electromagnetic compatibility of the conduction susceptibility of laser systems under the influence of different interference signals. Moreover, the wide application of integrated electronics causes complex electromagnetic environments, which makes the electromagnetic compatibility issues in

laser ranging systems increasingly challenging [29,30]. It is still uncertain which type of interference signal is more likely to cause electromagnetic interference to the laser ranging system. The reason for the electromagnetic sensitivity of the laser ranging systems is still unclear. From the system perspective, since the electromagnetic sensitivity of the system is unclear, and the external environment is complex and diverse, it is difficult to duplicate the real-time electromagnetic environment under the disturbed state of the equipment, leading to testing complexity, high cost and lack of accuracy [31,32]. Therefore, it is critical to study the susceptibility threshold of laser ranging systems with the injection of different interference signals and their electromagnetic sensitivity effects. Moreover, it is also significant to predict and evaluate the electromagnetic sensitivity of the laser ranging system in a complex electromagnetic environment. The bulk current injection method has great application in the study of the electromagnetic sensitivity characteristics of battery management system front-end integrated circuits and UAV positioning modules [33,34].

In this paper, we are the first to propose that electromagnetic interference can affect the normal operation of laser ranging systems. Moreover, we show that the propagation path of the interference signal uses the chip selection port of the laser sensing chip. Finally, we obtain the susceptibility threshold of the laser ranging system under the interference of different characteristic signals.

The rest of the sections are organized as follows. In Section 2, we start with a brief introduction to the operation principle of the laser ranging module. Section 3 presents an experimental platform establishing electromagnetic conduction susceptibility. In addition, the propagation path of electromagnetic interference and the type of interference signal are discussed. The measurement results and data analysis are presented in Section 4. Finally, in Sections 5 and 6, discussions and conclusions are presented.

2. Operation Principle of the Laser Ranging Module

In this work, a laser ranging system composed of a Vl53l0x laser ranging sensor module is considered. The main components of the laser ranging module include a detection array composed of single–photon avalanche diode, non-volatile memory, random access memory, read-only memory, microprocessor, advanced ranging core component related to the core algorithm and vertical cavity surface emitting laser. The transmitter emits a 940 nm laser signal to ensure the safety of the experimenters. Two laser echo signals are received by the receiver of the laser ranging module. One is the laser loop formed by the reflection of the laser emit caused by the transmitter when encountering the shelter; the other is the crosstalk loop caused by the glass plate on the surface of the laser module. To improve the optical immunity of the laser ranging module, a physical infrared filter thin cover glass was placed on the surface of the laser ranging module. The internal structure and schematic diagram of the laser ranging module are shown in Figure 1.

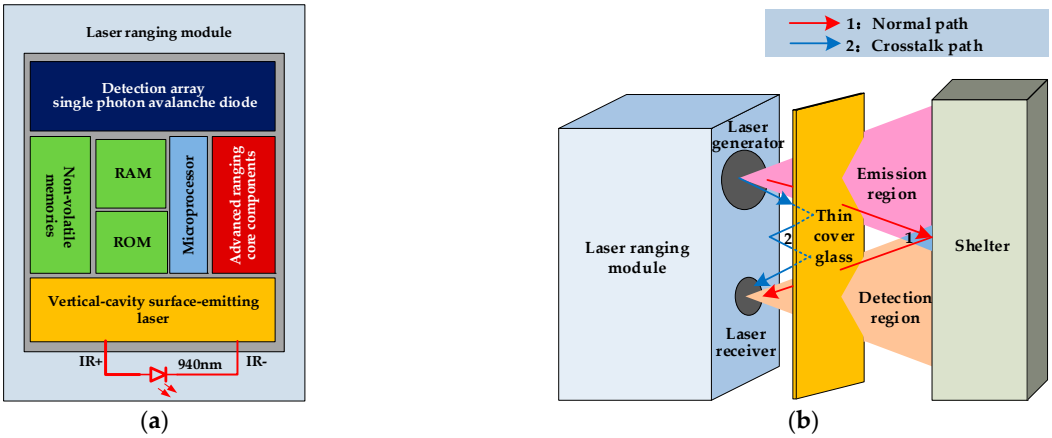

Figure 1. Laser ranging module: (**a**) the internal structure of the VL53L0X laser ranging sensor module; (**b**) schematic diagram.

Pulsed laser ranging technology is used in the laser ranging module. Firstly, the laser transmitter emits a periodic pulse laser signal, and then the detection array unit detects the diffuse reflection laser pulse signal of the occlusion. A pulse laser ranging system is usually composed of several modules: control module, laser emitting module, laser receiving module and time-interval measurement module. The circuit module composition of the laser ranging system is shown in Figure 2.

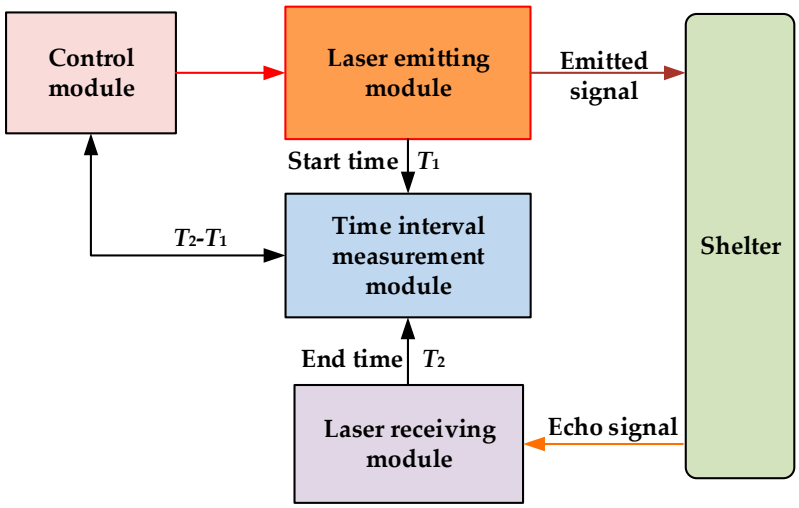

Figure 2. The circuit module composition of the laser ranging system.

T_1 and T_2 represent the time when the laser transmitter transmits the pulse signal and the receiver receives the echo signal, respectively. The shelter affects the time T_2, which in turn determines the distance from the shelter to the laser module. As the shelter moves away from the transmitter, the time T_2 taken for the echo signal received from the receiver becomes longer. Conversely, when the shelter is close to the transmitter, it takes less time T_2 to receive the echo signal from the receiver. Moreover, the laser ranging module has good performance within 3 m. Therefore, the effect of the distance between the shelter and laser module on the electromagnetic compatibility conducted susceptibility is not considered. The distance between the laser ranging module and the shelter is d, and the speed of light propagation in the air is about $c = 3.0 \times 10^8$ m/s. Therefore, the expression of the distance d measured by the laser ranging module is

$$d = \frac{c(T_2 - T_1)}{2} \tag{1}$$

The equivalent circuit of a pulsed semiconductor laser driving module can be regarded as being composed of a charging module, a switch control unit, an energy storage unit and a semiconductor laser device. The equivalent block diagram can be represented by an equivalent circuit. The equivalent circuit of a pulsed semiconductor laser driving module is shown in Figure 3.

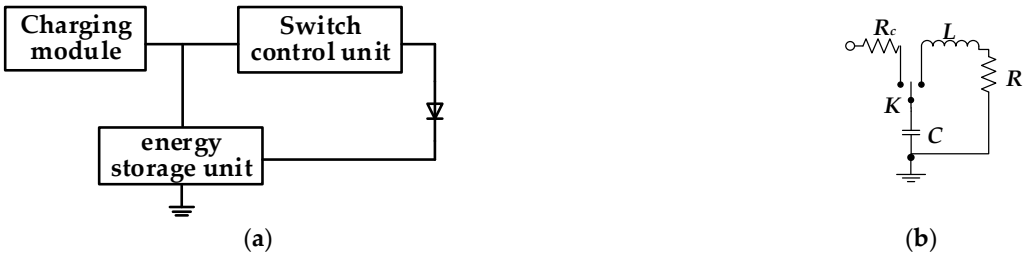

Figure 3. The equivalent circuit of a pulsed semiconductor laser driving module: (**a**) frame, (**b**) equivalent circuit.

In the equivalent circuit, C represents the energy storage module of the laser device, L represents the parasitic inductance generated by the whole system, and K is equivalent to the switching device when the avalanche diode discharges. The equivalent circuit of a pulse laser ranging system in a discharged state can be equivalent to a series of RLC circuits with zero input response. If the current of the equivalent discharge circuit is $i(t)$, the following equation can be obtained from Kirchhoff's Law of Voltage:

$$L\frac{di}{dt} + Ri + \frac{1}{C}\int i\mathrm{dt} = 0, \tag{2}$$

$$i(t) = Ae^{-\alpha t}\sin(\omega t + \theta), \tag{3}$$

$$\alpha = \frac{R}{2L}, \tag{4}$$

$$w = \sqrt{\frac{1}{LC} - (R/2L)^2}, \tag{5}$$

In Equation (2) to Equation (5), α represents the attenuation factor of the sine wave, A represents the current amplitude, and w represents the angular frequency of the current. In the pulse source, the pulse excitation current is determined by the first sine wave, and a large attenuation factor can make the pulse current attenuate faster, which can effectively protect the laser device. The smaller angular frequency w can ensure that the sine wave signal has a steep rising edge and a narrow pulse width.

3. Experiment

The electromagnetic sensitivity experiment of the laser ranging system was carried out in a microwave darkroom to reduce interference from the external electromagnetic environment. The whole electromagnetic sensitivity experiment system consisted of signal generator, signal combination device, typical circuit system sensitivity detection device, current injection device platform and several RF cables. The interference signal generated by the signal generator was injected into the laser ranging module of the sensitive detection device of the typical circuit system by the current probe after passing through the combiner and power amplifier in the signal combination device [35,36]. The signal combination device could input two interference signals at the same time through the S_1 port and the S_2 port. The typical circuit system sensitivity test device was a functional integration module that studies the influence of different interference signals on a typical circuit system. The laser ranging system was one of the modules in a typical circuit system. The laser sensor module in typical circuit-sensitive detection equipment emits the pulse laser signal through the transmitter, receives it through the sensitive receiving unit, and displays the detected distance value on the liquid crystal display (LCD) screen through the microcontroller unit (MCU). The two MCUs shown in Figure 4 were the same thing. The figure facilitates observation of the interference signals being injected into the specified cable. The MCU could process the data collected by the laser ranging module, and supply power to the enabling terminal of the laser ranging module. Interference signals were injected by the big current probe at the chip select enable port of the laser ranging module. The current monitor probe was located 5 cm from the laser ranging module and the injection probe was 5 cm from the current monitor probe. A block diagram of the electromagnetic sensitivity experiment of the laser ranging system is shown in Figure 4.

We conducted electromagnetic conduction sensitivity experiments and confirmed that electromagnetic interference can effectively interfere with the working state of the laser ranging system. Different types of interference signal were injected into the laser ranging system to explore the effects on electromagnetic sensitivity. Single-frequency signals, pulse amplitude modulation (AM) signals, triangular wave AM signals and pulse frequency modulation signals were used as interference signals in the conduction sensitivity tests.

The selection of these types of interference signal can expand the signal types in the CS114 standard. These interference signals can analyze the threshold and frequency of susceptibility and the effect of waveforms on the system. Electromagnetic Compatibility Conducted Susceptibility is usually significantly related to the power and time duty cycle of the interfering signal. By comparing these waveforms, the correlation between electromagnetic conduction sensitivity and time and power can be evaluated. The characteristics of each signal are shown in Table 1.

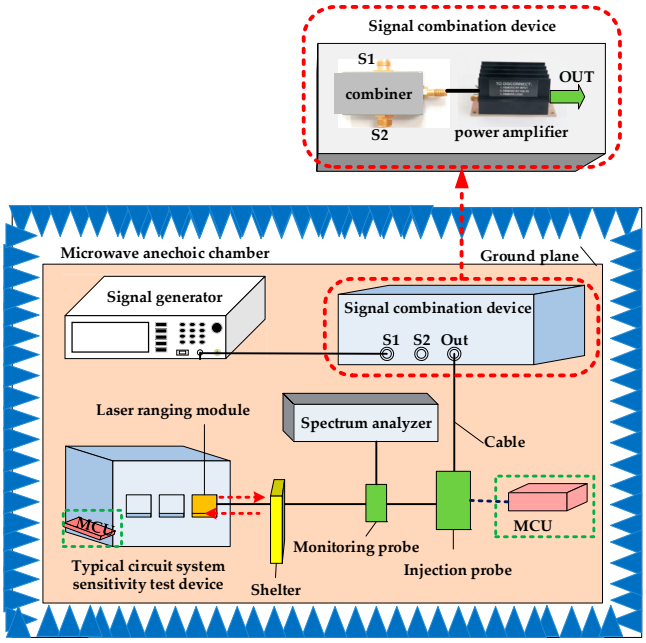

Figure 4. Block diagram of electromagnetic sensitivity experiment of the laser ranging system.

Table 1. Types and features of interference signal characteristics.

Interference Signals	Feature 1	Feature 2	Feature 3
single-frequency signal			
pulse AM signal	modulation depths	pulse period	duty cycles
triangular wave AM signal	modulation depths	Triangular wave periods	rising edge time
pulse frequency modulation signal	frequency offsets	pulse period	duty cycles

The steps of the injection of interference signals into the system are as follows. Firstly, the compatible positive voltage regulator provided a stable voltage VDD for the laser sensor chip to ensure the proper working of the laser sensor chip. Secondly, the single-frequency interference signal and three different modulation interference signals were generated by a radio frequency signal source. Thirdly, interference signals were injected by the large current probe at the chip to enable the porting of the laser ranging module. The port test circuit of the laser sensor chip is shown in Figure 5.

The shelter in front of the laser sensor was moved to change the distance between the shelter and the laser sensor. We observed whether the LCD value changed dynamically. The module circled in yellow is the laser ranging sensor chip. The electromagnetic sensitivity test platform of the laser ranging system is shown in Figure 6.

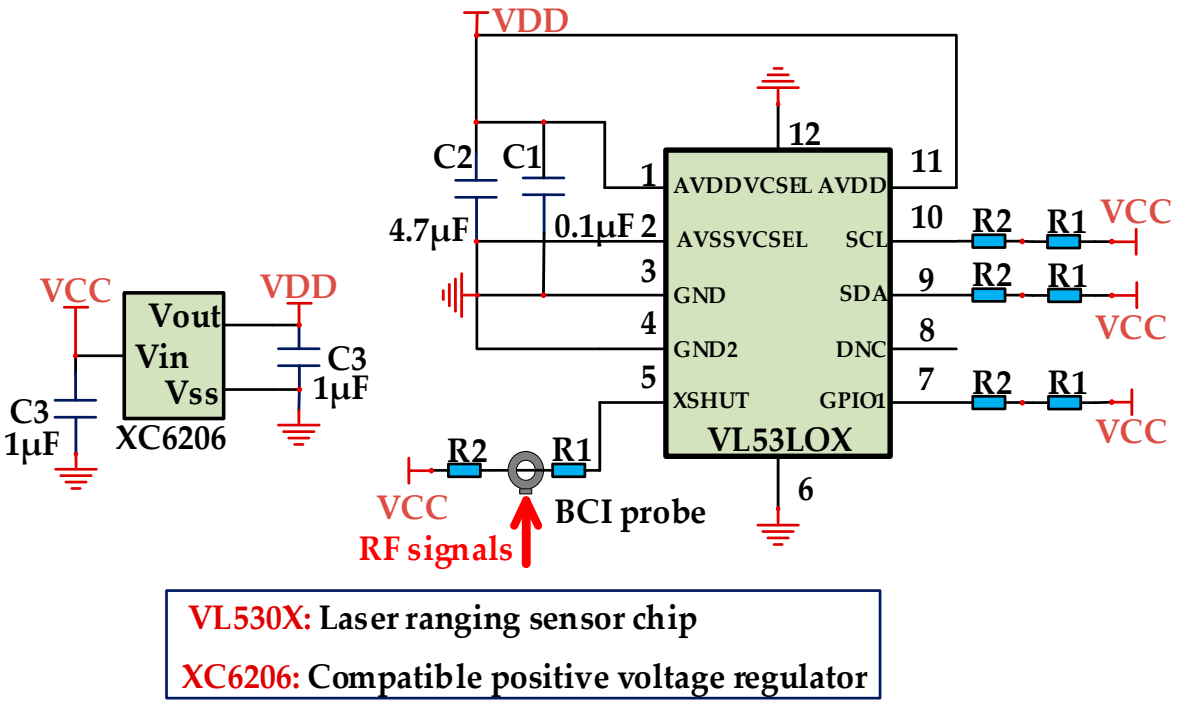

Figure 5. The port test circuit of the laser ranging sensor chip.

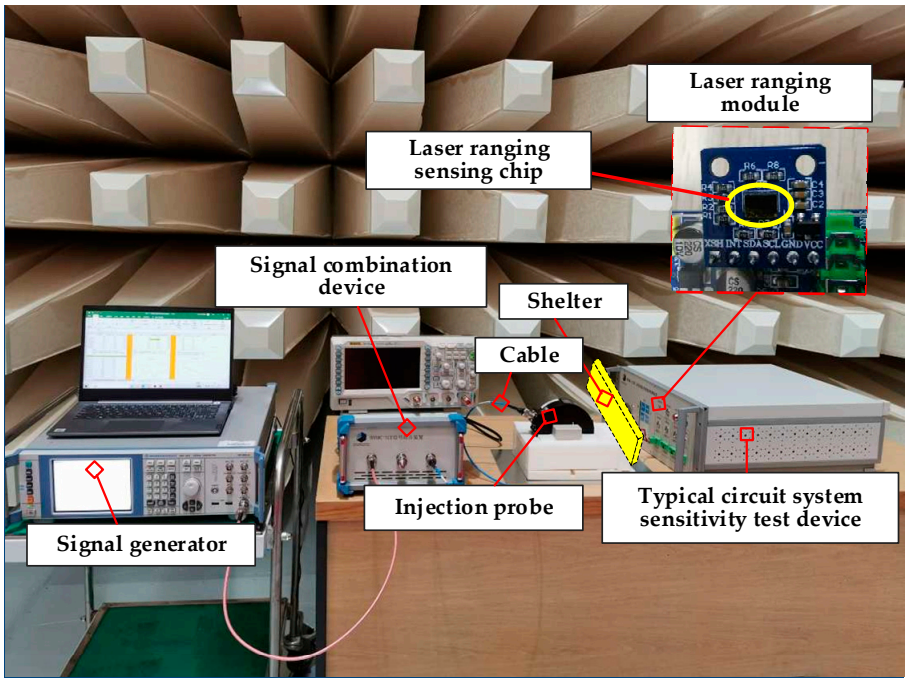

Figure 6. The electromagnetic sensitivity test platform of the laser ranging system.

4. Results

4.1. Effects of Electromagnetic Interference on Laser Ranging System

In an environment without electromagnetic interference, the distance value on the LCD changes in real-time when moving the shelter. However, the LCD values were constantly stuck when the strength of the interference signals increased beyond its susceptibility threshold. The system only worked properly after being restarted.

4.2. Characteristics of Laser Ranging System under Different Electromagnetic Interference Signals

Through the RF signal source, the single-frequency sinusoidal signal, pulse amplitude modulation signal, triangular wave amplitude modulation signal and pulse frequency modulation signal were injected into the laser ranging system, and the electromagnetic sensitivity characteristics of the laser ranging system under the different characteristic modes of four kinds of interference signals were analyzed. The output signal power value of the RF signal source was regarded as the susceptibility threshold of the system when the laser ranging system was not working properly.

The susceptibility threshold curve of the laser ranging system under single-frequency interference is shown in Figure 7. Figure 7 shows that, under the interference of a single-frequency signal in the frequency range of 10–60 MHz, the susceptibility threshold of the laser ranging system is less than −20 dBm, which makes it vulnerable to interference. In the single-frequency interference signal experiment, the susceptibility threshold of the band near 30 MHz was lower than that of other bands. Therefore, the 30 MHz sinusoidal signal was used as the carrier signal for the modulated signal. In the low and high-frequency bands, the susceptibility threshold of the laser ranging system was relatively large, and the anti-interference performance of the system was relatively strong.

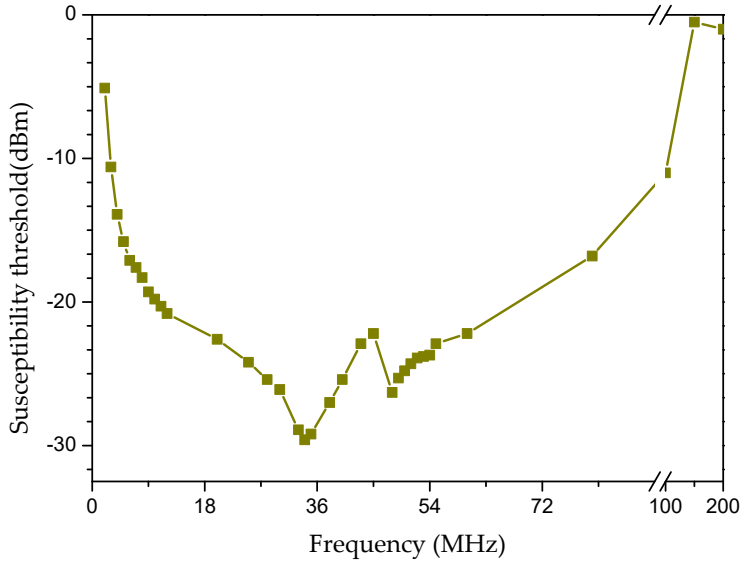

Figure 7. The susceptibility threshold curve of the laser ranging system under single-frequency interference.

In the study of the influence of pulse AM modulation interference signal on the laser ranging system, the susceptibility threshold curve of pulse AM modulation signal was studied under different modulation depths, different pulse cycle lengths and different pulse duty cycles. The susceptibility threshold curve of the laser ranging system under pulse AM modulation interference is shown in Figure 8.

The electromagnetic sensitivity experimental data in Figure 8 show that the susceptibility threshold curve of the laser ranging module tends to be stable at about −32 dBm under different duty ratios of the pulse-modulated signal, which indicates that the duty ratio of the pulse-modulated signal has little effect on the electromagnetic sensitivity of the laser ranging system. The susceptibility threshold curve of the laser ranging system is stable at −31.5 dBm with different pulse period lengths, which indicates that the pulse period lengths of the pulse modulation signal have little effect on the electromagnetic sensitivity of the system. At different modulation depths, the susceptibility threshold of the laser ranging system decreases with the increase in modulation depth, and is more vulnerable to interference.

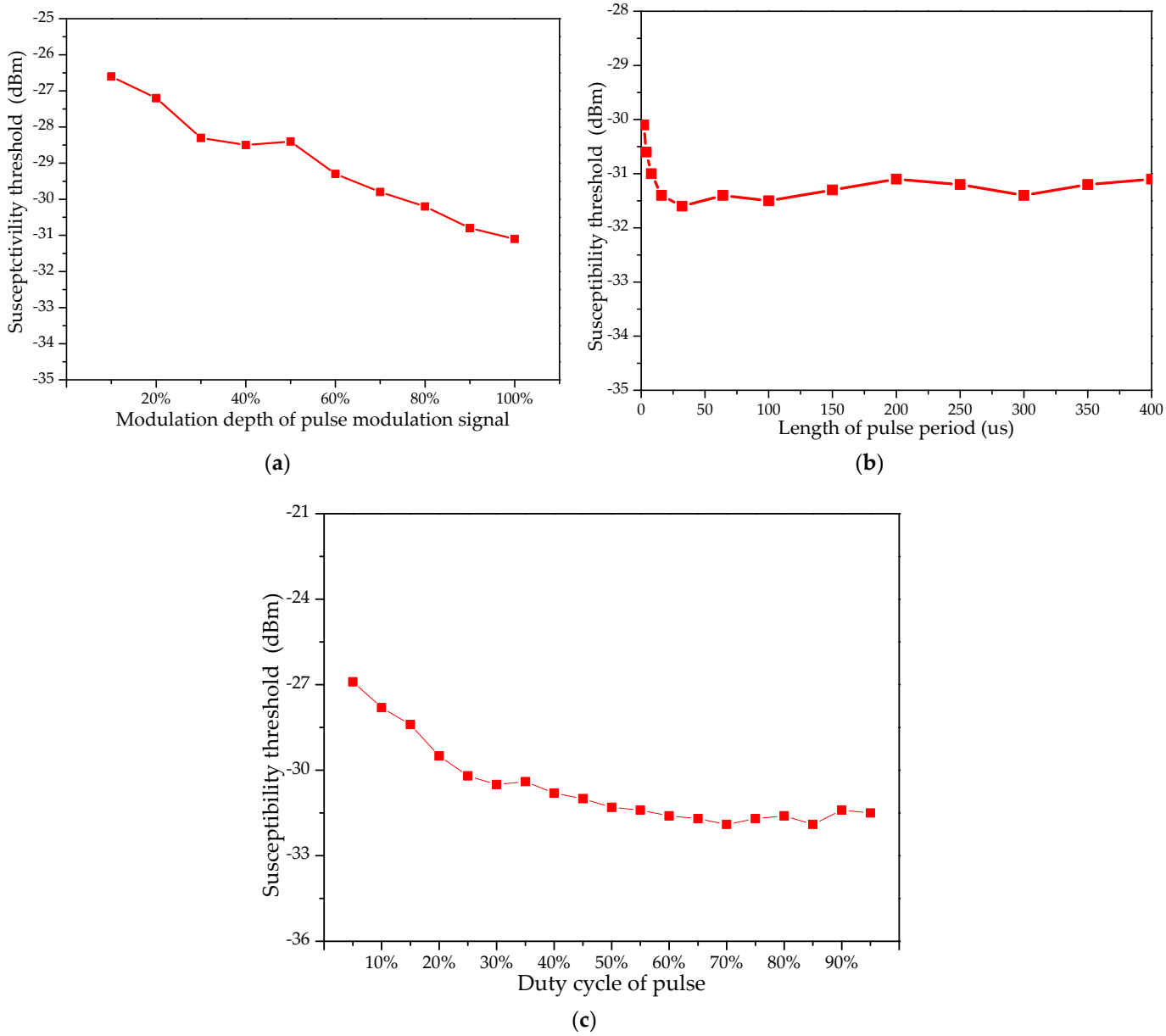

Figure 8. The susceptibility threshold curve of the laser ranging system under pulse AM modulation interference: (**a**) under different modulation depths; (**b**) under different pulse periods; (**c**) under different pulse duty cycles.

To explore the susceptibility threshold curve of the laser ranging system to the triangular wave AM modulation signal, this paper studied the triangular wave AM modulation signal under different periods and different rising edges. The rising edge of the triangular wave was 500 us, the modulation depth of the triangular wave modulation signal was 100%, and the carrier frequency was 30 MHz. The susceptibility threshold curve of the triangular wave modulation signal under different periods of triangular wave modulation signal is shown in Figure 9a, and the susceptibility threshold curve of the triangular wave modulation signal under different rising edges of triangular wave AM modulation signal is shown in Figure 9b. From the two figures, it can be seen that the change in modulation signal period and rising edge has no obvious effect on the electromagnetic sensitivity of the laser ranging system, and the susceptibility threshold of the laser ranging system is always about −27.8 dBm.

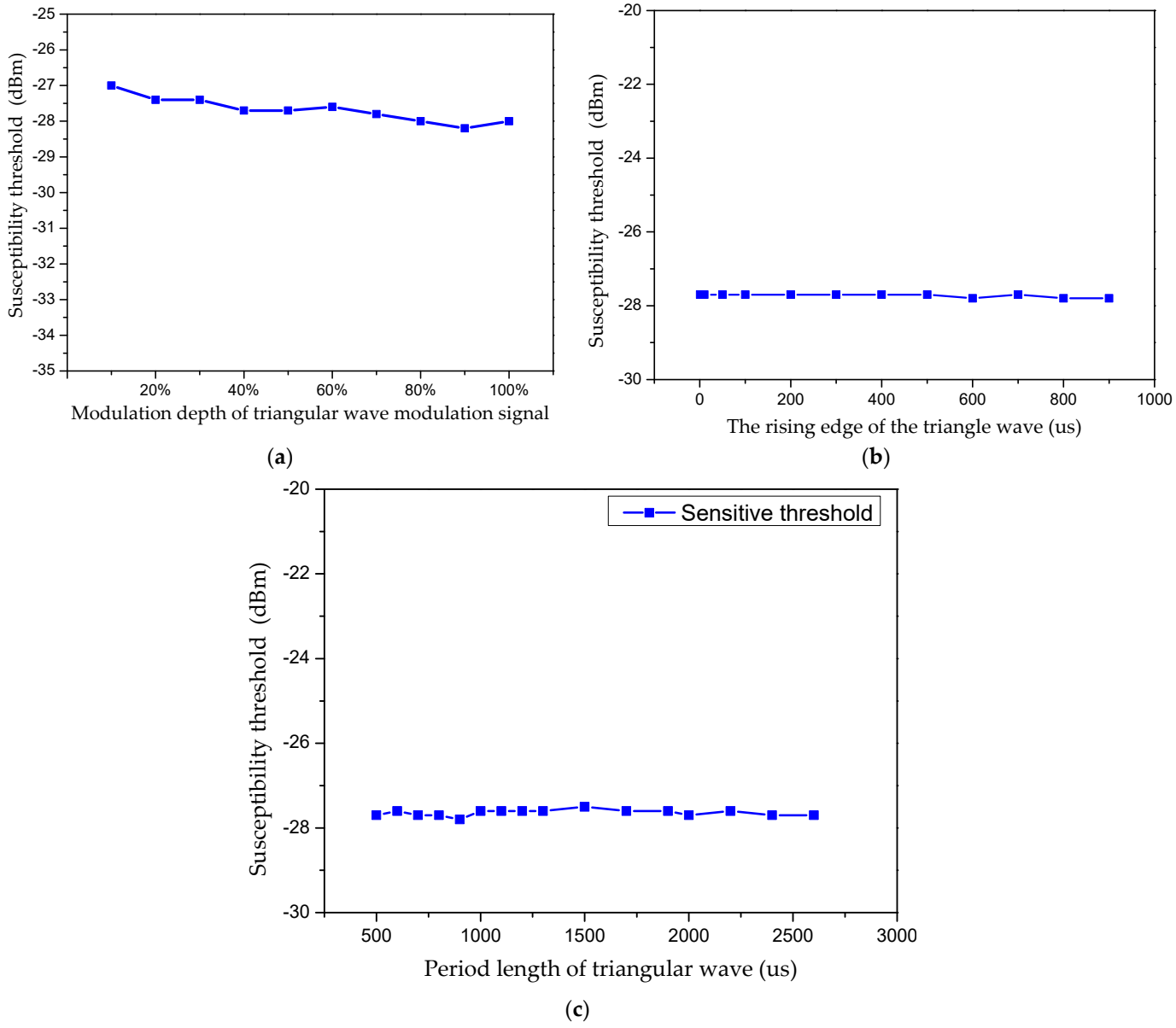

Figure 9. The susceptibility threshold curve of the laser ranging system under triangular wave AM modulation signals: (**a**) under different modulation depths; (**b**) under different rising edge times of triangular wave; (**c**) under different periods of triangular wave.

The relationship between the susceptibility threshold of the laser sensing system and the pulse frequency modulation interference signal is shown in Figure 10. The susceptibility threshold curve of the laser ranging system showed no obvious change under the influence of FM signal interference signals in terms of the three characteristics mentioned in Figure 10a–c. The susceptibility threshold of the laser ranging system was stable at −30 dBm under the interference of the FM signal.

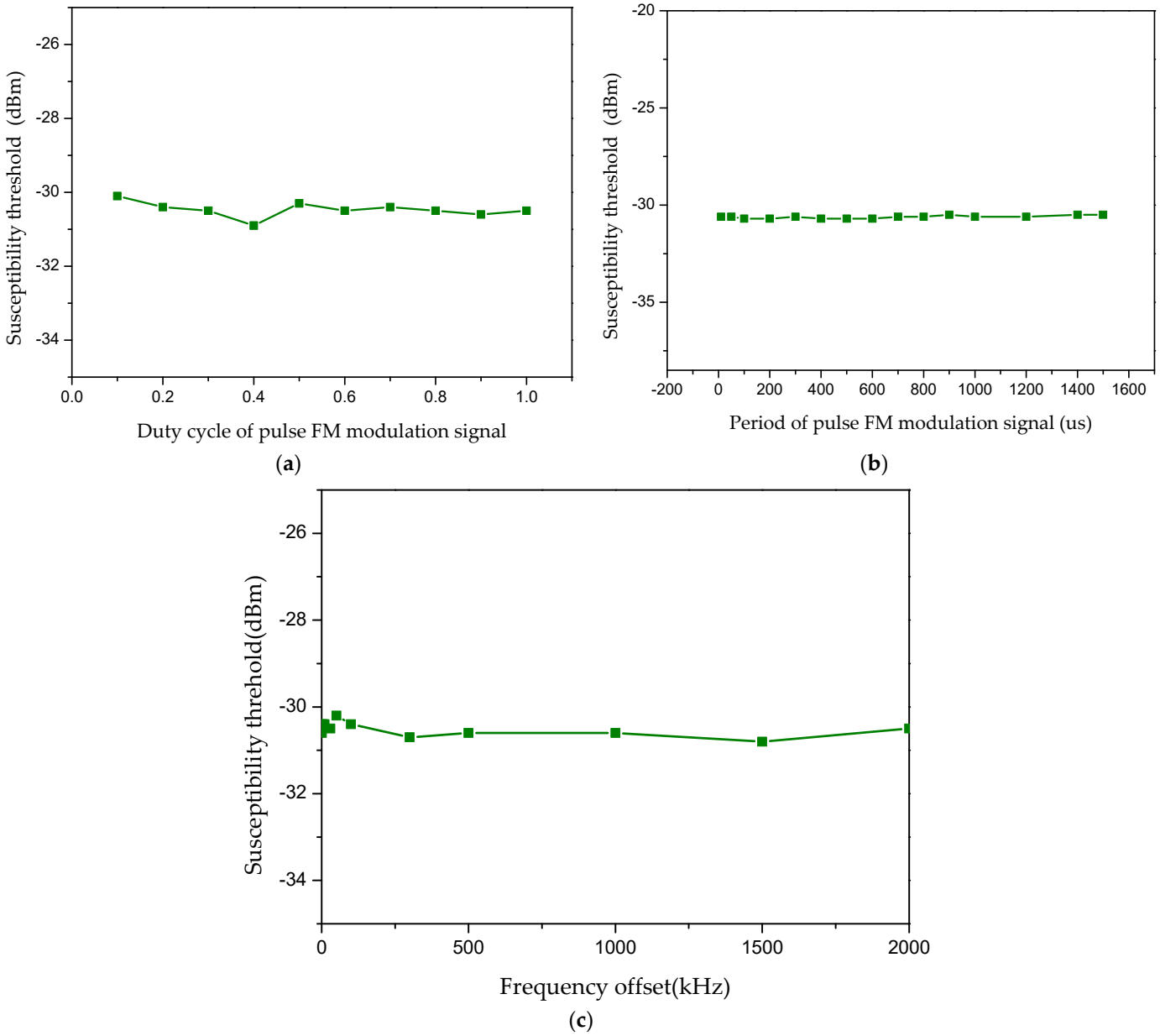

Figure 10. The susceptibility threshold curve of the laser sensing system under the interference of pulse frequency modulation signals: (**a**) under different duty cycles of pulse FM modulation signal; (**b**) under different period pulse FM modulation signals: (**c**) under different frequency offsets.

5. Discussion

With regard to the abnormal operation of laser ranging systems, we propose that the disturbance in the laser ranging system is probably caused by electromagnetic interference and confirm that electromagnetic interference can cause abnormalities in a laser ranging system by injecting a radio frequency interference signal into the chip selection start port of the laser ranging chip. Through an analysis of the chip port test circuit, it was found that the chip selection start port of the laser chip is subject to electromagnetic interference, which causes the normal working chip to be in the unselected idle state and results in the chip no longer working.

To further study the electromagnetic effect of the laser ranging system under different interference signals, we carried out a series of electromagnetic conduction sensitivity experiments and obtained a susceptibility threshold curve for the laser ranging system

under different interference signals. According to the experimental data, the laser ranging system was found to be more sensitive to the frequency and amplitude intensity of the interference signals.

This research on the electromagnetic sensitivity of laser ranging systems is of great significance for the rapid evaluation of laser ranging systems in complex electromagnetic environments, and also provides guidance for the design of laser ranging systems and laser ranging chips in the future.

6. Conclusions

In this paper, we analyzed the structure of a pulse laser ranging module, and the working principle of laser ranging, and revealed the electromagnetic sensitivity of a laser ranging system by using the electromagnetic compatibility conduction sensitivity experiment. By analyzing the susceptibility threshold curve of the laser ranging system under different interference signals, it was concluded that the laser ranging system is only sensitive to interference signals whose amplitude exceeds the susceptibility threshold. The stability of the susceptibility threshold of the system is independent of duty cycle, period, frequency offset and other characteristics of the interference signal. This method can comprehensively obtain the electromagnetic sensitive boundary of the laser system and the electromagnetic environment effect mechanism of the laser system can be inferred from the test results. This provides an effective way to assess the sensitivity characteristics of laser ranging systems in the future and provide theoretical support.

Author Contributions: P.H. and B.L. suggested and directed the project; D.S. provided theoretical support; W.L. and Y.L. helped to complete the experiments; P.H. wrote the original manuscript. All authors have read and agreed to the published version of the manuscript.

Funding: This research was funded by the National Natural Science Foundation of China under grant number 62293492 and 62293495, and the Shanghai Natural Science Fund under grant number 20ZR1454800.

Institutional Review Board Statement: Not applicable.

Informed Consent Statement: Not applicable.

Data Availability Statement: Not applicable.

Conflicts of Interest: The authors declare no conflict of interest.

References

1. Su, D.; Xie, S.; Dai, F.; Liu, Y.; Jia, Y. *The Theory and Methods of Quantification Design on System-Level Electromagnetic Compatibility*, 1st ed.; National Defense Industry Press: Beijing, China, 2015; pp. 71–83.
2. Su, D.; Xie, S.; Chen, A.; Shang, X.; Zhu, K.; Xu, H. Basic Emission Waveform Theory: A Novel Interpretation and Source Identification Method for Electromagnetic Emission of Complex Systems. *IEEE Trans. Electromagn. Compat.* **2018**, *60*, 1330–1339. [CrossRef]
3. Wu, Q.; Su, D. *Electromagnetic Compatibility Principles, Modeling and Design*, 1st ed.; The Posts and Telecommunications Press: Beijing, China, 2022; pp. 4–17.
4. Lee, J.; Kim, Y.-J.; Lee, K.; Lee, S.; Kim, S.-W. Time-of-flight measurement with femtosecond light pulses. *Nat. Photonics* **2010**, *4*, 716–720. [CrossRef]
5. Zhang, Z.; Xiao, Y.; Ma, Z.; Xiao, M.; Ding, Z.; Lei, X.; Karagiannidis, G.K.; Fan, P. 6G Wireless Networks: Vision, Requirements, Architecture, and Key Technologies. *IEEE Veh. Technol. Mag.* **2019**, *14*, 28–41. [CrossRef]
6. Zhong, K.; Zhou, X.; Huo, J.; Yu, C.; Lu, C.; Lau, A.P.T. Digital Signal Processing for Short-Reach Optical Communications: A Review of Current Technologies and Future Trends. *J. Light. Technol.* **2018**, *36*, 377–400. [CrossRef]
7. Poulton, C.V.; Byrd, M.J.; Russo, P.; Timurdogan, E.; Khandaker, M.; Vermeulen, D.; Watts, M.R. Long-Range LiDAR and Free-Space Data Communication with High-Performance Optical Phased Arrays. *IEEE J. Sel. Top. Quantum Electron.* **2019**, *25*, 7700108. [CrossRef]
8. Halterman, R.; Bruch, M. In Velodyne HDL-64E LIDAR for Unmanned Surface Vehicle Obstacle Detection. In Proceedings of the Conference on Unmanned Systems Technology XII, Orlando, FL, USA, 12–14 April 2010.

9. Abdo, J.; Hamblin, S.; Chen, G. Effective Range Assessment of Lidar Imaging Systems for Autonomous Vehicles under Adverse Weather Conditions with Stationary Vehicles. *ASCE-ASME J. Risk Uncert. Eng. Syst. Part B Mech. Eng.* **2021**, *8*, 031103. [CrossRef]
10. Kuutti, S.; Fallah, S.; Katsaros, K.; Dianati, M.; Mccullough, F.; Mouzakitis, A. A Survey of the State-of-the-Art Localization Techniques and Their Potentials for Autonomous Vehicle Applications. *IEEE Internet Things J.* **2018**, *5*, 829–846. [CrossRef]
11. Zhao, X.; Sun, P.; Xu, Z.; Min, H.; Yu, H. Fusion of 3D LIDAR and Camera Data for Object Detection in Autonomous Vehicle Applications. *IEEE Sens. J.* **2020**, *20*, 4901–4913. [CrossRef]
12. Ren, K.; Wang, Q.; Wang, C.; Qin, Z.; Lin, X. The Security of Autonomous Driving: Threats, Defenses, and Future Directions. *Proc. IEEE* **2020**, *108*, 357–372. [CrossRef]
13. Kaushal, H.; Kaddoum, G. Applications of Lasers for Tactical Military Operations. *IEEE Access* **2017**, *5*, 20736–20753. [CrossRef]
14. Sabatini, R.; Gardi, A.; Ramasamy, S.; Richardson, M.A. In A Laser Obstacle Warning and Avoidance system for Manned and Unmanned Aircraft. In Proceedings of the 2014 IEEE Metrology for Aerospace (Metro Aero Space), Benevento, Italy, 29–30 May 2014; pp. 616–621.
15. Lednev, V.N.; Grishin, M.Y.; Sdvizhenskii, P.A.; Kurbanov, R.K.; Litvinov, M.A.; Gudkov, S.V.; Pershin, S.M. Fluorescence Mapping of Agricultural Fields Utilizing Drone-Based LIDAR. *Photonics* **2022**, *9*, 963. [CrossRef]
16. Hong, D.; Gao, L.; Yokoya, N.; Yao, J.; Chanussot, J.; Du, Q.; Zhang, B. More Diverse Means Better: Multimodal Deep Learning Meets Remote-Sensing Imagery Classification. *IEEE Trans. Geosci. Remote Sens.* **2021**, *59*, 4340–4354. [CrossRef]
17. Yao, J. Microwave Photonics. *J. Light. Technol.* **2009**, *27*, 314–335. [CrossRef]
18. Jin, K.; Zhou, W. Wireless Laser Power Transmission: A Review of Recent Progress. *IEEE Trans. Power Electron.* **2019**, *34*, 3842–3859. [CrossRef]
19. Lin, H.S.; Han, H.W.; Ma, L.H.; Ding, Z.C.; Jin, D.D.; Zhang, X.H. Range Intensity Profiles of Multi-Slice Integration for Pulsed Laser Range-Gated Imaging System. *Photonics* **2022**, *9*, 505. [CrossRef]
20. Liu, S.; Zhan, H.; Peng, K.; Sun, S.; Li, Y.; Ni, L.; Wang, X.; Jiang, J.; Yu, J.; Zhu, R.; et al. Yb-Doped Aluminophosphosilicate Triple-Clad Laser Fiber with High Efficiency and Excellent Laser Stability. *IEEE Photonics J.* **2019**, *11*, 1501010. [CrossRef]
21. Wang, K.; Gu, H.; Yang, Y.; Wang, K.; Wang, Y. Impact of Application Characteristics on Laser Energy Fluctuation in Integrated Photonic Switching Systems. *IEEE Photonics J.* **2023**, *15*, 6600312. [CrossRef]
22. Pang, Y.; Xu, Y.; Zhao, X.; Qin, Z.; Liu, Z. Stabilized Narrow-Linewidth Brillouin Random Fiber Laser with a Double-Coupler Fiber Ring Resonator. *J. Light. Technol.* **2022**, *40*, 2988–2995. [CrossRef]
23. Song, E.; Zhu, G.; Wang, H.; Dong, J.; Qian, Y.; Aleksei, K.; Zhu, X. Minimizing Thermal Load and Stabilizing Mode in Yb:YAG Thin Disk Laser by 1030 nm Multi-Pass Pumping. *IEEE Photonics Technol. Lett.* **2020**, *32*, 1011–1014. [CrossRef]
24. Wan, Y.; Yang, B.; Xi, X.; Zhang, H.; Wang, P.; Wang, X.; Xu, X. Comparison and Optimization on Transverse Mode Instability of Fiber Laser Amplifier Pumped by Wavelength-Stabilized and Non-Wavelength-Stabilized 976 nm Laser Diode. *IEEE Photonics J.* **2022**, *14*, 1503905. [CrossRef]
25. Ying, K.; Chen, D.; Pi, H.; Wang, Z.; Li, X.; Sun, Y.; Wei, F.; Yang, F.; Cheng, N.; Ye, Q.; et al. Ultra-Stable Fiber Laser Based on Intracavity Dual Mode Self-Reference Mechanism. *J. Light. Technol.* **2022**, *40*, 3923–3929. [CrossRef]
26. Cui, Y.; Ye, X.; Shi, J.; Huang, W.; Zhou, Z.; Wang, M.; Chen, Z.; Wang, Z. Stable and Efficient Coupling of High-Power Continuous-Wave Laser with Uncooled Anti-Resonant Hollow-Core Fibers with End Caps. *IEEE Photonics J.* **2022**, *14*, 7909806. [CrossRef]
27. Wen, Y.; Wang, P.; Shi, C.; Yang, B.; Xi, X.; Zhang, H.; Wang, X. Experimental Study on Transverse Mode Instability Characteristics of Few-Mode Fiber Laser Amplifier under Different Bending Conditions. *IEEE Photonics J.* **2022**, *14*, 1539106. [CrossRef]
28. Soares, B.; Robalinho, P.; Guerreiro, A.; Frazao, O. Resilience to Passive Attacks of a Secure Key Distribution System Based on an Ultra-Long Fiber Laser Using a Bi-Directional EDFA. *Photonics* **2022**, *9*, 825. [CrossRef]
29. Fors, K.; Linder, S.; Nilsson, J.; Sterner, U. Effects of Platform EMI in Synchronized Cooperative Broadcast Systems. *IEEE Trans. Electromagn. Compat.* **2021**, *63*, 1856–1864. [CrossRef]
30. Omollo, N.; Van der Ven, J.K.; Vogt-Ardatjew, R.; Leferink, F. Ieee, Determining the Electromagnetic Environment on Board Ships for Risk-based Approach EMC Analysis. In Proceedings of the 2020 IEEE International Symposium on Electromagnetic Compatibility and Signal & Power Integrity Virtual Symposium (IEEE EMC+SIPI), Reno, NV, USA, 28 July–28 August 2020; pp. 666–670.
31. Migliaccio, M.; Gil, J.J.; Sorrentino, A.; Nunziata, F.; Ferrara, G. The Polarization Purity of the Electromagnetic Field in a Reverberating Chamber. *IEEE Trans. Electromagn. Compat.* **2016**, *58*, 694–700. [CrossRef]
32. Yin, B.; Chen, C.; Zuo, L.; Li, B.; Yuan, L.; He, Y. An Evaluation Method of Electromagnetic Interference Based on a Fast S-Transform and Time–Frequency Space Model. *IEEE Trans. Electromagn. Compat.* **2022**, *64*, 396–404. [CrossRef]
33. Aiello, O.; Crovetti, P. Characterization of the Susceptibility to EMI of a BMS IC for Electric Vehicles by Direct Power and Bulk Current Injection. *IEEE Lett. Electromagn. Compat. Pract. Appl.* **2021**, *3*, 101–107. [CrossRef]
34. He, K.; Yu, D.; Guo, B.; Chai, M.; Zhou, C.; Zhang, D. An Equivalent Dynamic Test System for Immunity Characterization of the UAV Positioning Module Using Bulk Current Injection Method. *IEEE Lett. Electromagn. Compat. Pract. Appl.* **2020**, *2*, 161–164. [CrossRef]

35. *GJB 151B-2013*; Electromagnetic Emission and Susceptibility Requirements and Measurements for Military and Subsystems. Electronic Information Foundation Department of the General Equipment Department of the Chinese People's Liberation Army: Beijing, China, 2013.
36. *MIL-STD-461G*; Requirements for the Control of Electromagnetic Interference Characteristics of Subsystems and Equipment. Department of Defense Interface Standard: Arlington, VA, USA, 2015.